

A GENERALIZED SECOND ORDER COMPENSATOR DESIGN FOR VIBRATION CONTROL OF FLEXIBLE STRUCTURES

Hyochoong Bang[†] and Brij N. Agrawal[‡]
Naval Postgraduate School
Monterey, California

Abstract

In this paper, a modified positive position feedback compensator design is presented for vibration control of flexible structures. The new method provides extended capability of controlling structural natural frequencies and damping. A similar compensator design where only rate sensors are available is also discussed. Analytical and experimental results are presented to verify the proposed method.

I. Introduction

Vibration control of flexible structures using second order compensators has been extensively discussed in the previous studies.¹⁻⁴ The use of dynamic compensators in structural vibration control has wide applications, especially, to feedback stabilization of flexible structural systems. The direct velocity feedback is an explicit method of increasing damping by active control actions.⁵ The main difficulties in the direct velocity feedback are the finite actuator dynamics and high frequency input signals which produce unbounded frequency responses. On the other hand, the compensator design of Ref. [2] the so-called Positive Position Feedback(PPF) is closely connected to the direct velocity feedback technique. It is truly a PPF only when the compensator frequency equals the vibration frequency.

It is generally recognized that the PPF has some advantages over the direct velocity feedback, especially when the actuator dynamics are considered. Also, the frequency response for the PPF, which is essentially based upon a second order low pass filter, is more stable. The stability condition in the PPF turns out to be independent of modeling uncertainties such as structural damping and actuator dynamics. One disadvantage of the PPF is the limited number of design parameters since the only control variable is the damping of the system. This is also true for the direct velocity feedback on the assumption that the velocity is the information available from the sensors. In general cases, it is

necessary to have control over the both damping and stiffness of the system for high damping and increased bandwidth of the response. For structures with quite low natural frequencies^{3,4}, it is not sufficient simply to increase damping irrespective of the undamped natural frequencies.

The system responses are governed by both damping and stiffness of the system. Therefore, the design requirements are usually specified in terms of both damping and natural frequency/bandwidth of the closed-loop system. In this study, the PPF based upon compensators is generalized to accompany modifications in stiffness as well as damping of the closed-loop system. The key idea of this approach is to directly utilize the position information from the sensor to build the associated control law. Since the PPF makes use of the compensator output which is usually provided by a position sensor output, the original position information is lost when it is transformed into velocity information. In the new approach, both the original position output from the sensor and the compensator output are combined into the feedback control law in the general form. This new approach enables us to have more flexibility in deciding desired closed-loop responses by increasing number of design parameters, i.e., feedback gains. More feedback gains imply more design freedom for optimal performance of the system.

Also, another new approach, which uses rate sensor information instead of position sensor, is developed with a stability criterion. In this control law, the rate sensor output is directly utilized to increase closed-loop damping, and it is fed into a compensator so that the compensator output contribute to increase stiffness of the system. The controlled performance of the new approach turns out to be essentially same as the PPF scheme. Both methods provide stabilizing feedback control laws subject to stability constraints and the flexibility of deciding dynamic characteristics via an increased number of design parameters. Depending upon the availability of sensors and the difficulty of implementation, either approach can be chosen to achieve the equivalent control objective.

Experimental demonstrations are performed to verify the proposed method. Actual implementation of the control laws are made by digital compensators.

II. Problem Description

For general second order vibrational systems, the

[†] Research Assistant Professor, Department of Aeronautics and Astronautics, Member AIAA

[‡] Professor, Department of Aeronautics and Astronautics, Associate Fellow AIAA

linearized equations of motion are described as

$$\begin{aligned} M\ddot{\mathbf{q}} + K\mathbf{q} &= F\mathbf{u} \\ \mathbf{y} &= L[\mathbf{q}^T, \dot{\mathbf{q}}^T]^T \end{aligned} \quad (1)$$

where M is the mass matrix, K stiffness matrix, \mathbf{q} generalized coordinate vector, F input influence matrix, and \mathbf{y} is the measurement vector with output matrix L . The above equations, by introducing modal damping, can be rewritten in terms of modal coordinates as follows

$$\begin{aligned} \ddot{\xi} + D\dot{\xi} + \Omega\xi &= \Phi^T F\mathbf{u} \\ \mathbf{y} &= L[\xi^T \Phi^T, \dot{\xi}^T \Phi^T]^T \end{aligned} \quad (2)$$

where ξ is modal state vector of length N_m , and Φ is a modal matrix which satisfies

$$\Phi^T M \Phi = I, \quad \Phi^T K \Phi = \text{diag}[\omega_i^2] \quad (3)$$

and

$\Omega \equiv$ modal frequency matrix ($N_m \times N_m$)

$$= \begin{bmatrix} \omega_1^2 & & & \\ & \omega_2^2 & & \\ & & \ddots & \\ & & & \omega_{N_m}^2 \end{bmatrix}$$

$D \equiv$ modal damping matrix ($N_m \times N_m$)

$$= \begin{bmatrix} 2\zeta_1\omega_1 & & & \\ & 2\zeta_2\omega_2 & & \\ & & \ddots & \\ & & & 2\zeta_{N_m}\omega_{N_m} \end{bmatrix}$$

where ω_i is i -th natural frequency and ζ_i is the i -th modal damping ratio. The control law design consists of finding the stabilizing input \mathbf{u} as a function of either the sensor output (\mathbf{y}) or the system state variables ($\mathbf{q}, \dot{\mathbf{q}}$). One of the useful structural control law design methods is the direct use of the sensor output for the actuator input. In other words,

$$\mathbf{u} = -G\mathbf{y} \quad (4)$$

where G is a gain matrix of appropriate size.

For a collocated rate sensor, the above equation can be rewritten as⁵

$$\mathbf{u} = -G\mathbf{y} = -GF^T\dot{\mathbf{q}}, \quad \mathbf{y} = F^T\dot{\mathbf{q}} \quad (5)$$

For a positive definite gain matrix ($G > 0$), the above control law stabilizes the system, decreasing the following Lyapunov function

$$U = \frac{1}{2}\mathbf{q}^T M \mathbf{q} + \frac{1}{2}\mathbf{q}^T K \mathbf{q} > 0$$

hence,

$$\dot{U} = -\dot{\mathbf{q}}^T FGF^T \dot{\mathbf{q}} < 0 \quad (6)$$

One of the key advantages of the above control law for the collocated actuator/sensor pair is the guaranteed stability in the presence of modeling uncertainties and nonlinearities. However, in the direct velocity feedback law, precise measurement of velocity is needed for closed-loop stability. In addition, neglected actuator dynamics can cause instability of the closed loop system under the direct velocity feedback¹.

In the usual digital control systems, when a velocity sensor is replaced by a position sensor, the following approximation is used

$$s\mathbf{y} \sim \frac{s}{\tau s + 1}\mathbf{y} \quad (7)$$

where s is the Laplace operator and τ is a small number. The stability guarantees are also affected by possible phase lag created in the closed loop. Therefore, the direct velocity feedback needs to be implemented cautiously.

On the other hand, in practical application, the velocity information is not easily available compared to other variables such as position and acceleration. For the case where a position sensor is used, the velocity information can be estimated. The finite difference technique is not attractive enough from the stability and noisy signal viewpoint. Analog compensators, which can estimate velocity information from position input, are generally preferred over the finite difference method. In some recent studies, analog compensators (or called tuning filters) are used to control vibration of flexible structures¹⁻⁴.

III. Compensator Design using Position Information

In this approach, the available sensor output is limited to position information. The recent use of *active structures* as sensory systems supports the idea of position/strain sensor as a reasonable choice. One of the popular methods, which has been reported in some recent literature, is so-called Positive Position Feedback (PPF)¹⁻⁴. Active damping action can be attained by introducing a compensator which converts position from a sensor into velocity so that the compensator output can be used as a control variable.

As in the most previous approaches, a special case of collocated sensor/actuator pair is assumed for many reasons. The measurement equation for a collocated position sensor is given by

$$\begin{aligned} \mathbf{y} &= F^T \mathbf{q} \\ &= F^T \Phi \xi \end{aligned} \quad (8)$$

Previous PPF Approach

The original PPF developed by Fanson and Caughey² is stated in the form

$$\begin{aligned}\ddot{\xi} + D\dot{\xi} + \Omega\xi &= C^T G \eta \\ \ddot{\eta} + D_c \dot{\eta} + \Omega_c \eta &= \Omega_c C \xi\end{aligned}\quad (9)$$

where the η is the compensator state vector of length N_f , C is the distribution matrix related to $F^T \Phi$ depending upon the number of actuators and number of modes to control, and G is a diagonal feedback gain matrix as follows

$$G \equiv \text{diagonal gain matrix}(N_f \times N_f)$$

$$= \begin{bmatrix} g_1 & & & \\ & g_2 & & \\ & & \ddots & \\ & & & g_{N_f} \end{bmatrix}$$

In addition, Ω_c and D_c are the corresponding compensator modal frequency and modal damping matrices, respectively. In order to achieve maximum damping efficiency, the compensator modal frequency matrix Ω_c is selected to match with Ω , i.e., the modal frequency matrix of the system. The above control law is verified both analytically and experimentally in the original work.² Furthermore, recent studies in Ref. [3-4] applied the same control law to a very low frequency system. The results indicate that significant amount of active damping is achievable by PPF.

The stability of the above system in Eq. (9) is not guaranteed, however. The closed-loop stability is subject to system dynamics and the feedback gains. Ref. [2] presents a stability condition for the PPF as

$$\Omega - C^T G C > 0 \quad (10)$$

where the inequality denotes positive definiteness of a matrix. It is noteworthy that the stability condition does not include the damping matrix of the structure, which usually represents an uncertainty factor. In spite of the stability constraint, the PPF is generally recognized as being robust, useful, and easy to implement.

One disadvantage of the PPF, however, as mentioned earlier, is the lack of control over the stiffness of the system. The output from a position sensor is not included in the control law. In order to change the stiffness as well as the damping, it is necessary to incorporate position output into the control law. This improves dynamic response, i.e., the bandwidth of the closed-loop system, especially for a low frequency system as in Ref. [3-4].

Modified PPF

Motivated by the original PPF, we propose a new generalized PPF as follows

$$\begin{aligned}\ddot{\xi} + D\dot{\xi} + \Omega\xi &= C^T G_v \eta - C^T G_p C \xi \\ \ddot{\eta} + D_c \dot{\eta} + \Omega_c \eta &= \Omega_c C \xi\end{aligned}\quad (11)$$

where the new positive definite feedback gain matrix G_p is introduced to make use of the direct output from the position sensor. Hence, the new control law makes use of both compensator output(η) and sensor output(ξ) to build a generalized control law. The stability condition for the new system in Eq. (11) can be derived in a similar way to the criterion in Eq. (10). By defining a new modal frequency matrix as

$$\bar{\Omega} = \Omega + C^T G_p C \quad (12)$$

the new stability condition is dictated as

$$\bar{\Omega} > 0, \quad \bar{\Omega} - C^T G C > 0 \quad (13)$$

The most significant difference between the two criteria in Eqs. (10) and (13) is that the modal frequency matrix Ω is replaced by a new matrix $\bar{\Omega}$. As long as the feedback gain matrix G_p is positive definite, the modified modal frequency matrix $\bar{\Omega}$ is guaranteed to be positive definite. For a collocated sensor/actuator system, the new feedback gain matrix G_p contributes to modifying the undamped frequencies of the system. In addition, the stability region prescribed by the inequality condition in Eq. (10) is extended by the additional feedback action, which resulted in the new modal frequency matrix $\bar{\Omega}$.

The closed-loop system which includes system dynamics and the compensator is represented in the form

$$\frac{d}{dt} \begin{Bmatrix} \eta \\ \dot{\eta} \\ \xi \\ \dot{\xi} \end{Bmatrix} = \begin{bmatrix} 0 & I & 0 & 0 \\ -\Omega - C^T G_p C & -D & C^T G & 0 \\ 0 & 0 & 0 & I \\ \Omega_f C & 0 & -\Omega_f & -D_f \end{bmatrix} \begin{Bmatrix} \eta \\ \dot{\eta} \\ \xi \\ \dot{\xi} \end{Bmatrix} \quad (14)$$

The above equation, for notational simplicity, is written as

$$\dot{\mathbf{x}} = \bar{A} \mathbf{x}, \quad \text{for } \mathbf{x}(0) \quad (15)$$

and the feedback gains in the stability condition, Eq. (13), satisfy

$$\lambda_i(\bar{A}) < 0, \quad i = 1, 2, \dots, N_m + N_f \quad (16)$$

where λ_i is the i -th eigenvalue of the closed-loop system matrix \bar{A} . It is evident that the new modified PPF provides us with increased flexibility in deciding closed-loop eigenvalues. The number of design parameters, i.e., feedback gains, is increased to the size of closed-loop matrix \bar{A} . For optimization of feedback gains, the new approach with an increased number of design parameters is an attractive choice compared to the original PPF.

IV. Compensator Design using Rate Information

Another control law, which is essentially similar to the PPF, can be derived when only rate sensors are available. The measurement equation for collocated rate sensors is described as

$$\begin{aligned} \mathbf{y} &= \mathbf{F}^T \dot{\mathbf{q}} \\ &= \mathbf{F}^T \Phi \dot{\xi} \end{aligned} \quad (17)$$

Using the above measurement equation, and motivated by the PPF, we suggest the following compensator based closed-loop system.

$$\begin{aligned} \ddot{\xi} + D\dot{\xi} + \Omega\xi &= C^T G \eta - C^T G_v C \dot{\xi} \\ \ddot{\eta} + D_c \dot{\eta} + \Omega_c \eta &= \Omega_c^{\frac{1}{2}} C \dot{\xi} \end{aligned} \quad (18)$$

where G is a diagonal gain matrix as in the previous section, and G_v is a positive definite gain matrix. As can be shown, the output from rate sensors is directly incorporated into the rate feedback form. In addition, the rate sensor output is adopted as an input to the compensator, so that the compensator output is used to change the stiffness of the closed-loop system. Thus, the above control law has a close connection to the previous modified PPF method in the sense that one can control both damping and stiffness of the system. The stability condition for the above control law is described as (see Appendix)

$$\tilde{D} - C^T G^{\frac{1}{2}} \Omega_c^{\frac{1}{2}} D_c^{-1} \Omega_c^{\frac{1}{2}} G^{\frac{1}{2}} C > 0 \quad (19)$$

where \tilde{D} is a closed-loop damping matrix

$$\tilde{D} = D + C^T G_v C > 0 \quad (20)$$

The new stability criterion is significantly different from the one for PPF in Eq. (8). The system damping matrix and stiffness matrix of the compensator are introduced into the criterion. From robustness viewpoint, the previous PPF is better than the approach suggested herein. Two sets of feedback gain matrices (G, G_v) are used as design parameters. In addition, the stability condition is dependent upon the damping matrix which raises a robustness issue. By assuming relatively small size of the modal damping matrix, D , of the system, the stability condition is mainly dictated by C, G_v , and the modal damping matrix D_c of the system. Hence, the robustness issue arising from the stability condition is minimized by incorporating direct velocity feedback into the feedback on the compensator output.

The above control law is simplified into a direct velocity/rate feedback when the compensator dynamics is eliminated. As the velocity/rate feedback gain G_v increases, the stability of the system is assured in proportion. This exactly matches with the modified PPF case, where the feedback gain matrix G_p plays the role of extending the stability region.

Depending upon the outputs available from sensors, one can use either the modified PPF or the alternative method suggested in this section.

V. Application

Analytical Results

Applications of the new control laws are made for a model system. A simple cantilevered beam in Fig. 1 is adopted as a model system, and the mathematical modeling was formulated by the finite element method. Three sets of piezoceramic sensor/actuator are assumed to be placed along the beam axis. The control objective is to control three modes, and three sets of second order compensator are designed. The modal damping ratio of the system is assumed to be 0.3% while the corresponding damping ratio for the compensator is chosen to be as high as 100%.

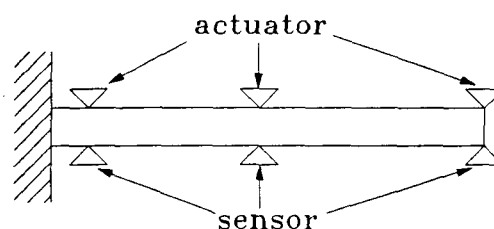


Figure 1 A cantilevered beam model

Based upon the model system and sensor/actuator setup, the closed-loop eigenvalues of the system are computed, and compared for the each control law. The results using position sensor output are presented in Table 1. As is shown in the table, the original PPF produces an unstable closed-loop system in accordance with the stability condition in Eq. (10). This instability is caused by the attempt to add too much damping just by using compensator output. Next, by the modified PPF which includes direct feedback on the position sensor output, the system is stabilized. In this case, the stability condition in Eq. (13) is satisfied by a modification of modal frequency matrix, which, in turn, increases the bandwidth of the system. The new feedback law, therefore, not only increases the stiffness, but also extends the stability region in this example. The new compensator is more effective than the original approach since one can control both damping and stiffness simultaneously, while the stability of the system is maintained.

Similar results using the control law of Eq. (12) are presented in Table 2. The instability, once again, is caused by the feedback on the compensator output only. Stability of the closed-loop system is achieved by making direct use of additional velocity feedback action

on the sensor output. In order to increase the stiffness of the system, the feedback gains on the velocity as well as the compensator output should be adjusted simultaneously.

Experimental Results

The previous analysis is further extended into experimental demonstrations. The experiment is limited to the PPF and modified PPF only since the sensor type is a position sensor. The experimental set-up is presented in Fig. 2. This Flexible Spacecraft Simulator (FSS) has been used for different applications of spacecraft maneuver and vibration control experiments^{3-4,6}. The main centerbody is attached to a flexible beam which represents a space antenna. The centerbody which is free to rotate on the airpads is fixed in this experiment to examine vibration control capability.

The flexible arm supported on the two airpads has its first mode natural frequency as low as 0.15Hz. The sensor and actuator used in this experiment are piezoceramics attached to the root of the beam as shown in Fig. 3. They are nearly collocated in order to prevent possible phase reversals between the sensor and actuator. The piezoceramics, when used as an actuator, produces bending moment over the element where the actuator is attached. On the other hand, when used as a sensor, it produces a voltage signal which is proportional to the charge developed over the piezoceramics, and thus to the strain of the sensor, which characterizes the sensor as a position sensor. The piezoceramic has been used to a large extent in the recent studies¹⁻⁴.

The compensator used in this study is a set of second order low pass filters described as

$$G_c^i(s) = \frac{\omega_c^2}{s^2 + 2\zeta_c\omega_c s + \omega_c^2}, \quad i = 1, 2, \dots, N_f \quad (21)$$

where the parameters(ω_c, ζ) are selected to produce maximum damping capability - the essential nature of tuning filters. For implementation of real time control, finite discretizations of the filter are achieved by one of the matching techniques called *backward difference*⁷

$$s = \frac{z-1}{Tz} \quad (22)$$

where z is the z -transform variable, and T is the sampling rate. Therefore, the digital compensator equivalent of Eq. (23) can be rewritten as

$$G_c^i(z) = \frac{T^2\omega_c^2 z^2}{(T^2\omega_c^2 + 1 + 2\zeta_c\omega_c T)z^2 - (2 + 2T\zeta_c\omega_c)z + 1}$$

The overall control block diagram including direct position feedback and compensators is presented in Fig. 4. A first order filter for the sensor output as in Fig. 4

is used to account for the phase lag of the output due to the discharge of piezoceramic when it is subject to low frequency excitations.

$$G_f(z) = \frac{\beta z}{\alpha z - 1} \quad (23)$$

where the filter parameters(α, β) are obtained experimentally.

Figures 5 and 6 show the results of the first mode control. Both natural vibration and vibration with active control are displayed. The original PPF is applied to control the first mode. It is shown that the active damping action is effective suppressing the vibration. Then, a modified PPF control action is examined to control the first mode. The results are provided in Fig. 6.

Figures 7 to 10 present results for both first and second modes excitation. Two independent digital tuning filters are generated and linearly combined into the necessary control input. The combinations should be made within the stability conditions in Eqs. (10) or (13). Figure 7 shows the case with the first mode tuning filter activated. The second mode is not properly controlled due to the nature of the tuning filter - a low pass filter tuned to the first mode. Results with the second mode tuning filter are presented in Fig. 8. In this case, while the second mode is effectively controlled, the first mode is not well controlled. Figure 9 represents results with both first mode and second mode tuning filters are activated. As expected, both modes are controlled effectively. Considering the actuator saturation limit $\pm 150V$ maximum during the considerable period of active damping, the damping action could have been more dramatic. Finally, the two tuning filters and direct position feedback are applied with the results presented in Fig. 10.

As was shown in the above, the tuning filters combined with direct position feedback provides more flexibility for selecting design parameters, i.e., feedback gains. In spite of the guaranteed stability of the system, the PPF or modified PPF do not provide optimal performance, in general. Further study on selecting the optimal set of feedback gains is necessary for performance improvement.

VI. Conclusions

A modified compensator-based control law design methodology is analyzed and verified experimentally. The new approach provides enhanced flexibility actively changing damping as well as stiffness of flexible structures. The stability region prescribed by the PPF is extended by the new approach. The analytical and experimental results demonstrate the advantages of the new compensator design.

Appendix

The closed-loop compensator and system equations are described as

$$\begin{aligned}\ddot{\xi} + D\dot{\xi} + \Omega\xi &= C^T G \dot{\eta} - C^T G_v C \dot{\xi} \\ \dot{\eta} + D_c \dot{\eta} + \Omega_c \eta &= \Omega_c^{\frac{1}{2}} C \dot{\xi}\end{aligned}\quad (A.1)$$

The above system is asymptotically stable if and only if the following condition is satisfied

$$\tilde{D} - C^T G^{\frac{1}{2}} \Omega_c^{\frac{1}{4}} D_c^{-1} \Omega_c^{\frac{1}{4}} G^{\frac{1}{2}} C > 0 \quad (A.2)$$

where \tilde{D} is a closed-loop damping matrix

$$\tilde{D} = D + C^T G_v C > 0 \quad (A.3)$$

Proof:

First, let us introduce a coordinate transformation in such a way that

$$\eta = G^{\frac{-1}{2}} \Omega_c^{\frac{1}{4}} \eta_t \quad (A.4)$$

where η_t is a new transformed coordinate. The above transformation is motivated by Fanson and Caughey's work.² Also, the subsequent proof is based upon the development in Ref. [2]. Substitution of Eq. (A.4) into Eq. (A.1) yields

$$\begin{aligned}\ddot{\xi} + \tilde{D}\dot{\xi} + \Omega\xi &= C^T G^{\frac{1}{2}} \Omega_c^{\frac{1}{4}} \dot{\eta}_t \\ \dot{\eta}_t + D_c \dot{\eta}_t + \Omega_c \eta_t &= \Omega_c^{\frac{1}{4}} G^{\frac{1}{2}} C \dot{\xi}\end{aligned}\quad (A.5)$$

or in a matrix form,

$$\begin{Bmatrix} \ddot{\xi} \\ \dot{\eta}_t \end{Bmatrix} + \begin{bmatrix} \tilde{D} & -E \\ -E^T & D_c \end{bmatrix} \begin{Bmatrix} \dot{\xi} \\ \dot{\eta}_t \end{Bmatrix} + \begin{bmatrix} \Omega & 0 \\ 0 & \Omega_c \end{bmatrix} \begin{Bmatrix} \xi \\ \eta_t \end{Bmatrix} = \mathbf{0} \quad (A.6)$$

where the matrix E is introduced as

$$E = C^T G^{\frac{1}{2}} \Omega_c^{\frac{1}{4}}$$

It should be noticed that all the coefficient matrices are symmetric. For stability proof, a positive definite Lyapunov function is taken as

$$V = \frac{1}{2} [\dot{\xi}^T, \dot{\eta}_t^T] \begin{bmatrix} \dot{\xi} \\ \dot{\eta}_t \end{bmatrix} + \frac{1}{2} [\xi, \eta_t]^T \begin{bmatrix} \Omega & 0 \\ 0 & \Omega_c \end{bmatrix} \begin{bmatrix} \xi \\ \eta_t \end{bmatrix} > 0 \quad (A.7)$$

Obviously, the Lyapunov function, being positive definite, has an equilibrium point at the origin. Now let us take time derivative of the Lyapunov function, and make use of Eq. (A.7). The result is

$$\dot{V} \equiv \frac{d}{dt} V = -[\dot{\xi}^T, \dot{\eta}_t^T] \begin{bmatrix} \tilde{D} & -E \\ -E^T & D_c \end{bmatrix} \begin{bmatrix} \dot{\xi} \\ \dot{\eta}_t \end{bmatrix} \quad (A.8)$$

For asymptotic stability, \dot{V} should be negative definite. In other words,

$$\dot{V} = -[\dot{\xi}^T, \dot{\eta}_t^T] \begin{bmatrix} \tilde{D} & -E \\ -E^T & D_c \end{bmatrix} \begin{bmatrix} \dot{\xi} \\ \dot{\eta}_t \end{bmatrix} < 0, \text{ for } [\dot{\xi}, \dot{\eta}_t] \neq \mathbf{0} \quad (A.9)$$

The above expression is expanded as

$$-x_1^T \tilde{D} x_1 - x_2^T D_c x_2 + x_1^T E x_2 + x_2^T E^T x_1 < 0 \quad (A.10)$$

where, for notational simplicity, $[x_1, x_2] \equiv [\dot{\xi}, \dot{\eta}_t]$ is introduced. Furthermore,

$$\begin{aligned}-x_1^T \tilde{D} x_1 - x_2^T D_c x_2 + x_1^T E x_2 + x_2^T E^T x_1 \\ + x_1^T E D_c^{-1} E^T x_1 - x_1^T E D_c^{-1} E^T x_1 < 0\end{aligned}\quad (A.11)$$

where we added and subtracted $x_1^T E D_c^{-1} E^T x_1$. In addition,

$$\begin{aligned}-x_1^T \tilde{D} x_1 + x_1^T E D_c^{-1} E^T x_1 - x_1^T E D_c^{-\frac{1}{2}} D_c^{-\frac{T}{2}} x_1 \\ + x_1^T E D_c^{-\frac{T}{2}} D_c^{\frac{1}{2}} x_2 + x_2^T D_c^{\frac{1}{2}} D_c^{-\frac{T}{2}} E^T x_1 - x_2^T D_c^{\frac{T}{2}} D_c^{\frac{1}{2}} x_2 < 0\end{aligned}\quad (A.12)$$

Combining each term, we obtain

$$\begin{aligned}-x_1^T (\tilde{D} - E D_c^{-1} E^T) x_1 \\ - (D_c^{-\frac{T}{2}} E^T x_1 - D_c^{\frac{1}{2}} x_2)^T (D_c^{-\frac{T}{2}} E^T x_1 - D_c^{\frac{1}{2}} x_2) < 0\end{aligned}$$

The second term in the above equation is always non-positive. Hence, for stability, the first term should be always negative to make \dot{V} negative definite. Hence, the stability condition is

$$\tilde{D} - E D_c^{-1} E^T > 0 \quad (A.13)$$

Substituting E

$$\tilde{D} - C^T G^{\frac{1}{2}} \Omega_c^{\frac{1}{4}} D_c^{-1} \Omega_c^{\frac{1}{4}} G^{\frac{1}{2}} C > 0 \quad (A.14)$$

References

- Goh, C.J., and Caughey, T.K., "On the Stability Problem Caused by Finite Actuator Dynamics in the Collocated Control of Large Space Structures", *International Journal of Control*, Vol. 41, No.3, 1985, pp. 787-802
- Fanson, J.L., and Caughey, T.K., "Positive Position Feedback Control of Large Space Structures", *Proceedings of the 28th AIAA Dynamics Specialists Conference* (Monterey, CA), AIAA, Washington, D.C., 1987, pp. 588-598
- Agrawal, B.N., Bang, H., and Hailey, J., "Application of Piezoelectric Actuators and Sensors in the Vibration Control of Flexible Spacecraft Structures", IAF 92-0319, World Space Congress, Washington, D.C., 28 Aug. - 5 Sept. 1992

- ⁴ Agrawal, B.N., and Bang, H., "Active Vibration Control of Flexible Space Structures by using Piezoelectric Sensors and Actuators", *Proceedings for 14th Biennial ASME Conference*, Albuquerque, Sept. 19-22, 1993, pp. 169-179
- ⁵ Balas, M.J., "Feedback Control of Flexible Systems", *IEEE Transactions on Automatic Control*, Vol. AC-23, No. 4, 1978, pp. 673-679
- ⁶ Newman, S.M., "Active Damping Control of a Flexible Space Structure using Piezoelectric Sensors and Actuators", Master's Thesis, Naval Postgraduate School, Monterey, CA, December, 1992
- ⁷ Phillips, C.L., and Nagle, Jr., H.T., *Digital Control System Analysis and Design*, Prentice-Hall, Inc., Englewood Cliffs, N.J., 1984

Table 1 Open and closed-loop eigenvalues for PPF

Open Loop($\times 10^2$)	Original PPF($\times 10^2$)	New PPF($\times 10^2$)
-0.0779-0.0000i	0.0245-0.0000i	-0.0275-0.0000i
-0.0002-0.0779i	-0.0316-0.1305i	-0.0433-0.0000i
-0.0002+0.0779i	-0.0316+0.1305i	-0.1108+0.0000i
-0.0779+0.0000i	-0.1437-0.0000i	-0.0496-0.1594i
-0.4883-0.0000i	0.2730+0.0000i	-0.0496-0.1594i
-0.0015-0.4883i	-0.0175-0.4991i	-0.0203-0.7145i
-0.0015+0.4883i	-0.0175+0.4991i	-0.0203+0.7145i
-0.4883+0.0000i	-1.0353-0.1993i	-0.8577-0.0000i
-1.3676-0.0000i	-1.0353+0.1993i	-1.0863+0.0000i
-1.3676+0.0000i	-0.0968-1.4900i	-1.5866-0.0000i
-0.0041-1.3676i	-0.0968+1.4900i	-0.0136-2.9182i
-0.0041+1.3676i	-1.6707+0.0000i	-0.0136+2.9182i

Table 2 Open and closed-loop eigenvalues for rate feedback

Open Loop($\times 10^2$)	With zero G_v ($\times 10^2$)	With nonzero G_v ($\times 10^2$)
-0.0779-0.0000i	-0.0582-0.0000i	-0.0561-0.0000i
-0.0002-0.0779i	0.0015-0.0788i	-0.0096-0.0786i
-0.0002+0.0779i	0.0015+0.0788i	-0.0096+0.0786i
-0.0779+0.0000i	-0.1121+0.0000i	-0.1383+0.0000i
-0.4883-0.0000i	0.2302-0.0000i	-0.1564-0.0000i
-0.0015-0.4883i	0.0175-0.4875i	-0.2454-0.4432i
-0.0015+0.4883i	0.0175+0.4875i	-0.2454+0.4432i
-0.4883+0.0000i	0.3682-1.0166i	-0.1274-0.6734i
-1.3676-0.0000i	0.3682+1.0166i	-0.1274+0.6734i
-1.3676+0.0000i	-1.2971-0.1384i	-1.3626-0.0530i
-0.0041-1.3676i	-1.2971-0.1384i	-1.3626+0.0530i
-0.0041+1.3676i	-1.6589-0.0000i	-4.2922-0.0000i

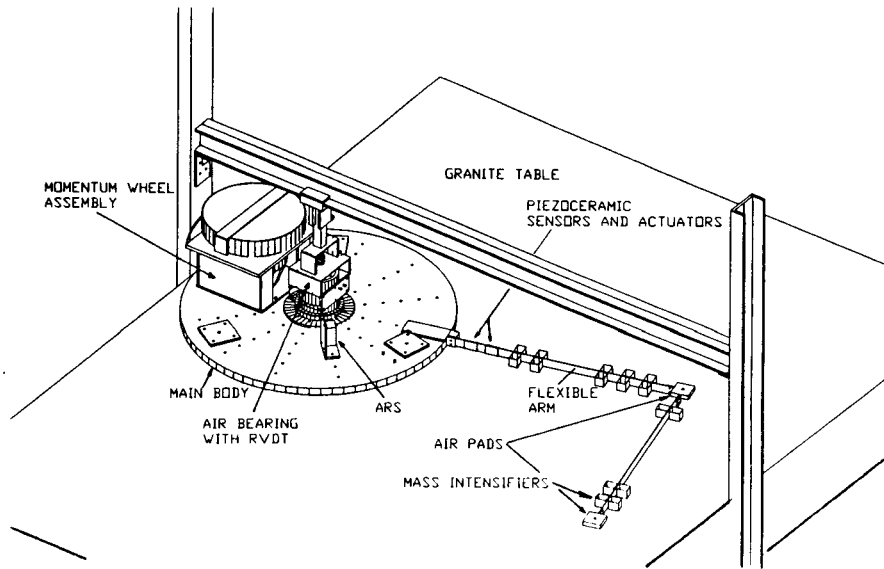


Figure 2 Flexible Spacecraft Simulator(FSS)

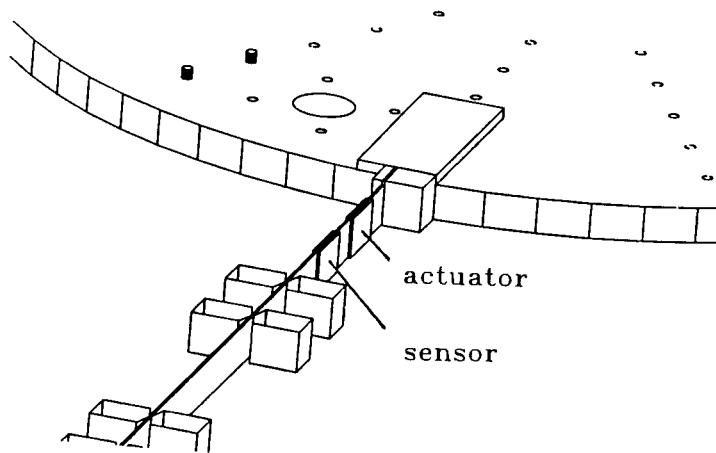


Figure 3 Piezoceramic sensor and actuator placement

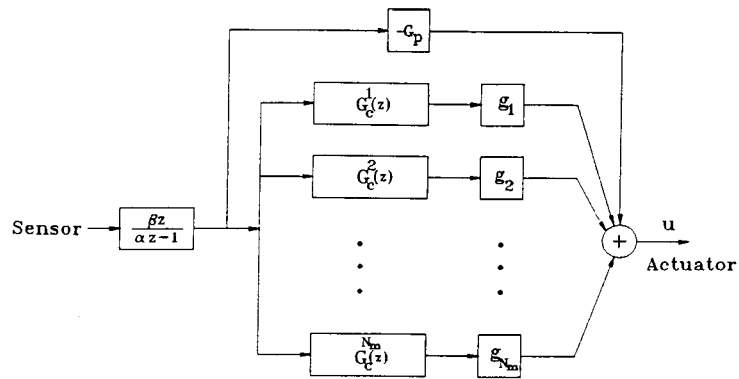


Figure 4 Digital compensator block diagram

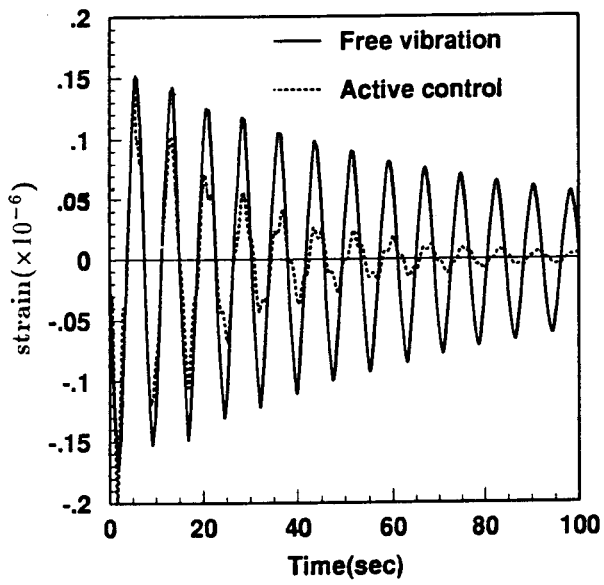


Figure 5 First mode vibration and active control

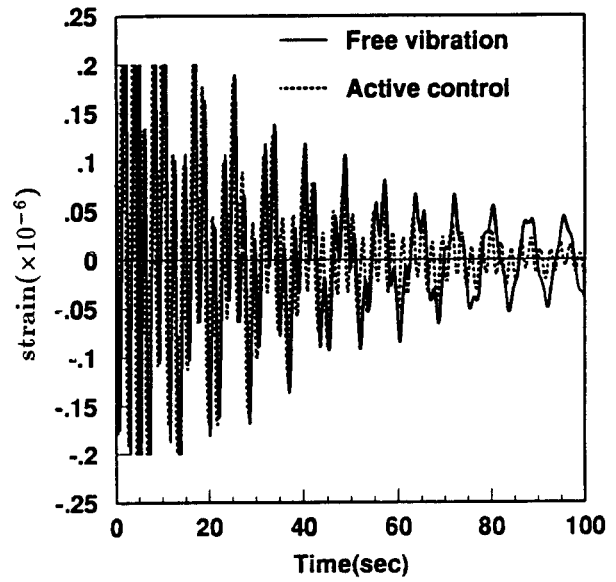


Figure 7 Multi-mode vibration and active first mode control

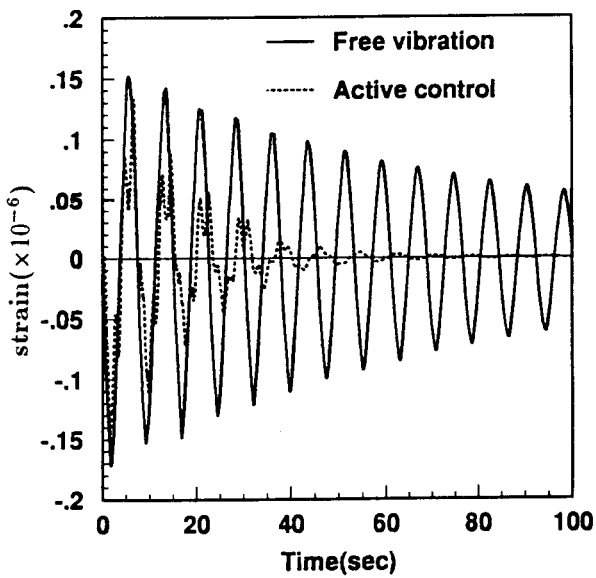


Figure 6 Modified PPF for first mode control

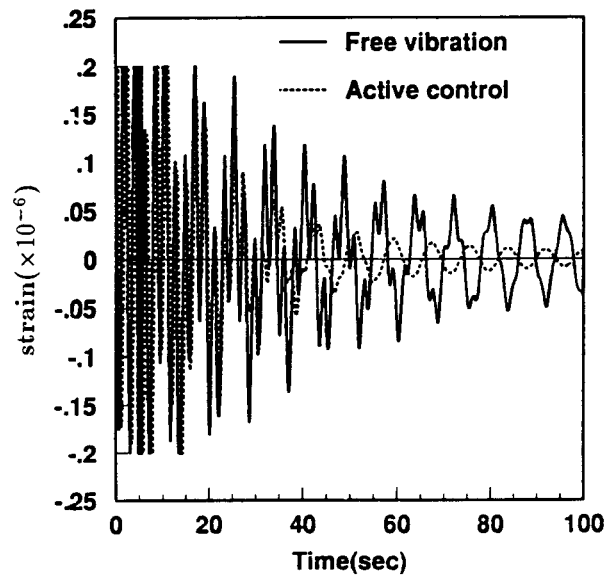


Figure 8 Multi-mode vibration and active second mode control

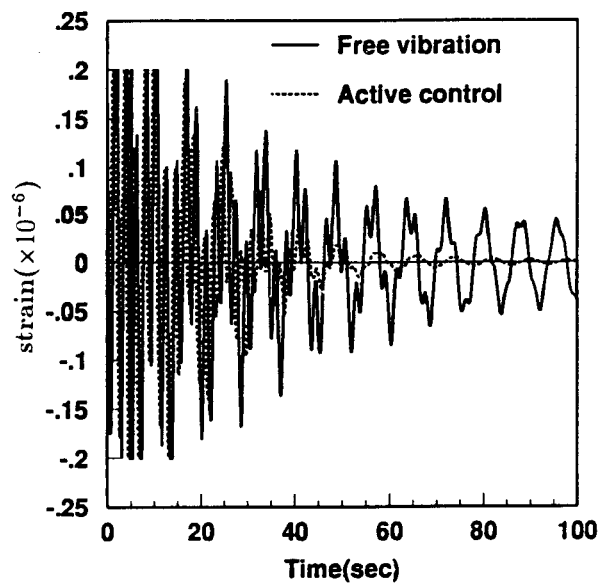


Figure 9 First and second mode control

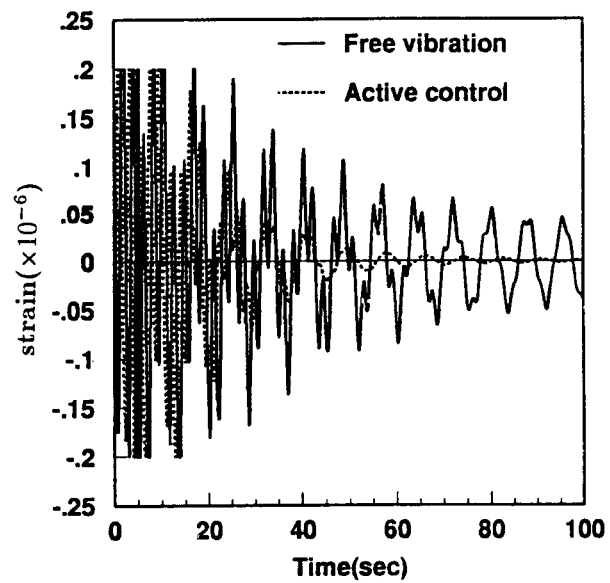


Figure 10 Modified PPF with active first and second mode control